

Statistical characterization of erosion and sediment transport mechanics in shallow tidal environments. Part 2: suspended sediment dynamics

Davide Tognin¹, Andrea D'Alpaos¹, Luigi D'Alpaos¹, Andrea Rinaldo², and Luca Carniello³

¹University of Padova

²École Polytechnique Fédérale de Lausanne EPFL

³Department of Civil, Environmental, and Architectural Engineering, University of Padova

December 7, 2022

Abstract

A proper understanding of sediment transport dynamics, critically including resuspension and deposition processes of suspended sediments, is key to the morphodynamics of shallow tidal environments.

Aiming to account for deposition mechanics in a synthetic theoretical framework introduced to model erosion dynamics (D'Alpaos et al., 2022), here we investigated suspended sediment dynamics.

A complete spatial and temporal coverage of suspended sediment concentration (SSC) required to effectively characterize re-suspension events is hardly available through observation alone, even combining point measurements and satellite images, but it can be retrieved by properly calibrated and tested numerical models.

We analyzed one-year-long time series of SSC computed by a bi-dimensional, finite-element model in six historical configurations of the Venice Lagoon in the last four centuries.

Following the peak over threshold theory, we statistically characterized suspended sediment dynamics by analyzing interarrival times, intensities and durations of overthreshold SSC events.

Our results confirm that, as for erosion events, SSC can be modeled as a marked Poisson process in the intertidal flats for all the considered historical configurations of the Venice Lagoon because exponentially distributed random variables well describe interarrival times, intensity and duration of overthreshold events.

Moreover, interarrival times, intensity and duration describing local erosion and overthreshold SSC events are highly related, although not identical because of the non-local dynamics of suspended sediment transport related to advection and dispersion processes.

Owing to this statistical characterization of SSC events, it is possible to generate synthetic, yet realistic, time series of SSC for the long-term modeling of shallow tidal environments.

1 **Statistical characterization of erosion and sediment**
2 **transport mechanics in shallow tidal environments.**
3 **Part 2: suspended sediment dynamics**

4 **Davide Tognin^{1,2}, Andrea D’Alpaos^{2,3}, Luigi D’Alpaos¹, Andrea Rinaldo^{1,2,4},**
5 **and Luca Carniello^{1,2}**

6 ¹Department of Civil, Environmental, and Architectural Engineering, University of Padova, Padova, Italy

7 ²Center for Lagoon Hydrodynamics and Morphodynamics, University of Padova, Padova, Italy

8 ³Department of Geosciences, University of Padova, Padova, Italy

9 ⁴Laboratory of Ecohydrology ECHO/IEE/ENAC, Ècole Polytechnique Fèdèrale de Lausanne, Lausanne,
10 Switzerland

11 **Key Points:**

- 12 • Exponential random variables well describe interarrival time, intensity and dura-
13 tion of resuspension events in tidal environments
- 14 • Similarly to erosion events, overthreshold resuspension events can be modelled as
15 marked Poisson processes over time
- 16 • Suspended sediment concentration and erosion dynamics are highly correlated but
17 differ due to advection and dispersion processes

Corresponding author: Davide Tognin, davide.tognin@unipd.it

Abstract

A proper understanding of sediment transport dynamics, critically including resuspension and deposition processes of suspended sediments, is key to the morphodynamics of shallow tidal environments. Aiming to account for deposition mechanics in a synthetic theoretical framework introduced to model erosion dynamics (A. D'Alpaos et al., Companion paper), here we investigated suspended sediment dynamics. A complete spatial and temporal coverage of suspended sediment concentration (SSC) required to effectively characterize resuspension events is hardly available through observation alone, even combining point measurements and satellite images, but it can be retrieved by properly calibrated and tested numerical models. We analyzed one-year-long time series of SSC computed by a bi-dimensional, finite-element model in six historical configurations of the Venice Lagoon in the last four centuries. Following the peak over threshold theory, we statistically characterized suspended sediment dynamics by analyzing interarrival times, intensities and durations of overthreshold SSC events. Our results confirm that, as for erosion events, SSC can be modeled as a marked Poisson process in the intertidal flats for all the considered historical configurations of the Venice Lagoon because exponentially distributed random variables well describe interarrival times, intensity and duration of overthreshold events. Moreover, interarrival times, intensity and duration describing local erosion and overthreshold SSC events are highly related, although not identical because of the non-local dynamics of suspended sediment transport related to advection and dispersion processes. Owing to this statistical characterization of SSC events, it is possible to generate synthetic, yet realistic, time series of SSC for the long-term modeling of shallow tidal environments.

1 Introduction

Suspended sediment dynamics in shallow tidal systems play a significant role as they influence geomorphic and ecological processes, that ultimately determine the long-term morphodynamic evolution of coastal, estuarine and lagoonal landscapes (Woodroffe, 2002; Masselink et al., 2014). Physical processes that drive sediment resuspension and transport in tidal environments are influenced by different hydrodynamic and sedimentological factors over a wide range of spatial and temporal scales.

Both tide and waves represent key drivers controlling sediment entrainment and transport in shallow tidal environments (Wang, 2012). The tide rise and fall generate

50 currents that propagate along the preferential pathways provided by the channel net-
51 work (Hughes, 2012) but, as the tide overflows on the adjoining intertidal flats, it is strongly
52 affected by shallower water and friction effects (Friedrichs & Madsen, 1992), so that its
53 velocity and, hence, its resuspension capacity can diminish considerably. Whereas, wind
54 waves with a typically short period can generate wave-orbital motions capable of resus-
55 pending intertidal-flat sediments (Anderson, 1972; Dyer et al., 2000; Carniello et al., 2005;
56 Green, 2011). Therefore, stochastic wave-forced resuspension can increase locally, mainly
57 under storm conditions, and can overcome the cyclic resuspension by tidal currents in
58 generating high turbidity (Green et al., 1997; Ralston & Stacey, 2007; Sanford, 1994).
59 Wave-driven resuspension and erosion together with tide- and wave-driven sediment trans-
60 port give rise to mechanisms leading to basin-wide sediment movement, which strongly
61 shape the morphology of shallow tidal systems (e.g., Nichols & Boon, 1994; Green & Coco,
62 2007; Carniello et al., 2011; Green & Coco, 2014). The repeated cycles of erosion, resus-
63 pension and deposition, that sediments may undergo, winnow fine particles from coarser
64 ones and, thus, modify sediment distribution and textural properties of intertidal flats
65 and subtidal platforms, influencing physical and biological processes (Dyer, 1989), light
66 climate (Moore & Wetzel, 2000) and ecosystem productivity (Carr et al., 2010; Lawson
67 et al., 2007; Carr et al., 2016; McSweeney et al., 2017).

68 Moreover, resuspension dynamics are mutually linked to numerous biological and
69 ecological processes (Temmerman et al., 2007; Kirwan & Murray, 2007; A. D'Alpaos et
70 al., 2007, 2011; Marani et al., 2013). Benthic vegetation and algae play a key role in in-
71 creasing sediment stability of subtidal platforms (Nepf, 1999; Tambroni et al., 2016; Ve-
72 nier et al., 2014). In fact, the interaction of flexible vegetation and bedforms can reduce
73 the effective bed shear stress and, consequently, sediment mobility. Similarly, the action
74 of halophytic vegetation over salt marshes has a significant impact on landscape devel-
75 opment, enhancing accretion, both by directly trapping inorganic sediment and by pro-
76 ducing organic matter (Marani et al., 2013; A. D'Alpaos & Marani, 2016; Roner et al.,
77 2016). However, some studies have also suggested that, although vegetation anchors sed-
78 iment through rooting and by slowing water flows, erosion and scour of the proximal sed-
79 iments can also be enhanced (Temmerman et al., 2007; Tinoco & Coco, 2016). Microal-
80 gae, although small, may also heavily impact sediment erodability. Indeed, extracellu-
81 lar polymeric secretions (EPS) of microphytobenthos can increase grain adhesion and
82 consequently erosion threshold of the sedimentary substrate (Le Hir et al., 2007; Par-

83 sons et al., 2016; Chen et al., 2019). As a result, sediment resuspension decreases in the
84 presence of EPS, which affects light availability and, in turn, microalgae proliferation,
85 thus triggering positive feedback (Pivato et al., 2019). Benthic fauna can further mod-
86 ify the bed sediment by changing its geotechnical properties and erosion resistance (Widdows
87 & Brinsley, 2002; Vu et al., 2017).

88 Owing to the complexity of the underlying processes and the interplay between phys-
89 ical and biological drivers, sediment dynamics in shallow tidal systems are rather entan-
90 gled. Therefore, observation-based approaches have been widely adopted to investigate
91 the suspended sediment concentration (hereafter SSC), using either in situ point mea-
92 surements (e.g., Wren et al., 2000; Gartner, 2004; Brand et al., 2020) or remote sensing
93 and satellite image analysis (Miller & McKee, 2004; Ruhl et al., 2001; Volpe et al., 2011).
94 However, both these techniques have some drawbacks. In situ measurements can pro-
95 vide an accurate description of the temporal dynamics of SSC, but lacks information on
96 its spatial heterogeneity. Moreover, acoustic and optical sensors installed in point tur-
97 bidity stations require periodic cleaning to prevent failure due to biofouling. Whereas,
98 satellite-based data can supply instantaneous information on SSC spatial variability, but
99 are barely informative on its temporal dynamics. Indeed, SSC events can hardly be fully
100 captured by satellites with fixed and often long revisit periods. Furthermore, intense SSC
101 typically occurs during severe storms, frequently characterized by clouds, which make
102 satellite data useless. As a matter of fact, reliable long-term SSC time-series at basin scale,
103 required for the statistical analysis performed herein, are seldom available.

104 In order to overcome these shortcomings and to exploit measurements of in situ
105 point observations and satellite images, these data can be combined to calibrate and test
106 numerical models (Ouillon et al., 2004; Carniello et al., 2014; Maciel et al., 2021), thereby,
107 using them as physically-based “interpolators” to compute temporal and spatial SSC dy-
108 namics. However, computing SSC dynamics over time scales of centuries in order to model
109 the morphodynamic evolution of tidal environments through fully-fledged numerical mod-
110 els is rather difficult owing to the computational burden involved. Therefore, modeling
111 the long-term evolution of tidal systems requires comprehending the physics of the pro-
112 cesses in order to properly characterize them in the framework of simplified approaches
113 (Murray, 2007).

114 Pointing to the development of a synthetic theoretical framework to represent in-
115 tense SSC events and to account for their landscape-forming action on tidal basin mor-
116 phology, we applied a two-dimensional finite element model to simulate the interaction
117 among wind waves, tidal current and sediment transport in several historical configu-
118 rations of the Venice Lagoon. In particular, we used a previously-calibrated and widely-
119 tested Wind Wave-Tidal Model (WWTM) (Carniello et al., 2005, 2011) coupled with
120 a sediment transport model (Carniello et al., 2012) to investigate hydrodynamics and
121 suspended sediment dynamics in the following six historical configurations of the Venice
122 Lagoon: 1611, 1810, 1901, 1932, 1970, and 2012. For each of them, we run a one-year-
123 long simulation forced with representative tidal and meteorological boundary conditions.
124 The computed SSC time series have been analyzed on the basis of the peak over thresh-
125 old (POT) theory, following the approach introduced by A. D’Alpaos et al. (2013) and
126 expanding the analysis performed by Carniello et al. (2016) to study the statistics of SSC
127 in the present configuration of the Venice Lagoon.

128 This study aims to expand this analysis to other historical configurations of the Venice
129 Lagoon (Figure 1) in order to unravel the effects on sediment transport of the morpho-
130 logical and anthropogenic modifications experienced by the lagoon in the last four cen-
131 turies and to test whether SSC dynamics can be modeled as a marked Poisson process
132 also when accounting for the morphological evolution of the basin. The latter represents
133 an interesting goal, being the use of stochastic frameworks particularly promising for long-
134 term studies, as pointed out by their increasing popularity in hydrology and geomorphol-
135 ogy to describe the long-term behaviour of geophysical processes (e.g., Rodriguez-Iturbe
136 et al., 1987; D’Odorico & Fagherazzi, 2003; Botter et al., 2013; Park et al., 2014; Bertas-
137 sello et al., 2018). Nonetheless, applications to tidal systems are still quite uncommon
138 (A. D’Alpaos et al., 2013; Carniello et al., 2016). Our analysis provides a spatial and tem-
139 poral characterization of resuspension events for the Venice Lagoon from the beginning
140 of the seventeenth century to the present, in order to show how morphological modifi-
141 cation affected sediment transport and to set a stochastic framework to forecast future
142 scenarios.

143 **2 Materials and Methods**

144 The Venice Lagoon (Figure 1) underwent different morphological changes over the
145 last four centuries, in particular due to anthropogenic modifications (L. D’Alpaos, 2010;

146 Finotello et al., 2022). From the beginning of the fifteenth century, the main rivers (Brenta,
147 Piave, and Sile) were gradually diverted in order to flow directly into the sea and pre-
148 vent the lagoon from silting up, but this triggered a sediment starvation condition. Later,
149 during the last century, the inlets were provided with jetties and deep navigation chan-
150 nels were excavated to connect the inner harbour with the sea (L. D’Alpaos, 2010; Sar-
151 retta et al., 2010). The jetties deeply changed the hydrodynamics at the inlets establish-
152 ing an asymmetric hydrodynamic behaviour responsible for a net export of sediment to-
153 ward the sea (Martini et al., 2004; Finotello et al., 2022), especially during severe storm
154 events, which are responsible for the resuspension of large sediment volumes (Carniello
155 et al., 2012). In general, these modifications heavily influenced sediment transport trig-
156 gering strong erosion processes that were further aggravated by sea-level rise. The net
157 sediment loss clearly emerges from the comparison among the different surveys of the
158 Venice Lagoon, which show a generalized deepening of tidal flats and subtidal platforms
159 as well as a reduction of salt-marsh area (Carniello et al., 2009). Indeed, in the last cen-
160 tury, the average tidal-flat bottom elevation lowered from -0.51 m to -1.49 m above mean
161 sea level (a.m.s.l.), while the salt-marsh area progressively shrank from 164.36 km² to
162 42.99 km² (Tommasini et al., 2019). Moreover, repeated closures of storm-surge barri-
163 ers designed to protect the city of Venice from flooding and known as Mo.S.E. system
164 are expected to further exacerbate this morphological degradation by cutting off signif-
165 icant supplies of inorganic sediments brought in by intense storm-surge events (Tognin
166 et al., 2022).

167 To study the influence of these morphological changes on suspended sediment dy-
168 namics, we considered six different historical configurations of the Venice Lagoon, rang-
169 ing from the beginning of the seventeenth century to today (Figure S1). The three most
170 ancient configurations (i.e. 1611, 1810, and 1901) were modeled by relying on histori-
171 cal maps, whereas the topographic surveys carried out by the Venice Water Authority
172 (Magistrato alle Acque di Venezia) in 1932, 1970, and 2003 were used for the more re-
173 cent ones (L. D’Alpaos, 2010; Finotello et al., 2022). Due to some morphological mod-
174 ifications at the three inlets associated with the Mo.S.E. system and almost completed
175 in 2012, the 2003 configuration was updated, so we will refer to this configuration as the
176 2012 configuration. For a detailed description of the methodology applied for the recon-
177 struction of the historical configurations of the Venice Lagoon and additional informa-
178 tion on the more recent bathymetric data, we refer the reader to Tommasini et al. (2019).

179 Further details on the geomorphological setting and the implications on erosion and re-
 180 suspension events are reported in A. D'Alpaos et al. (Companion paper).

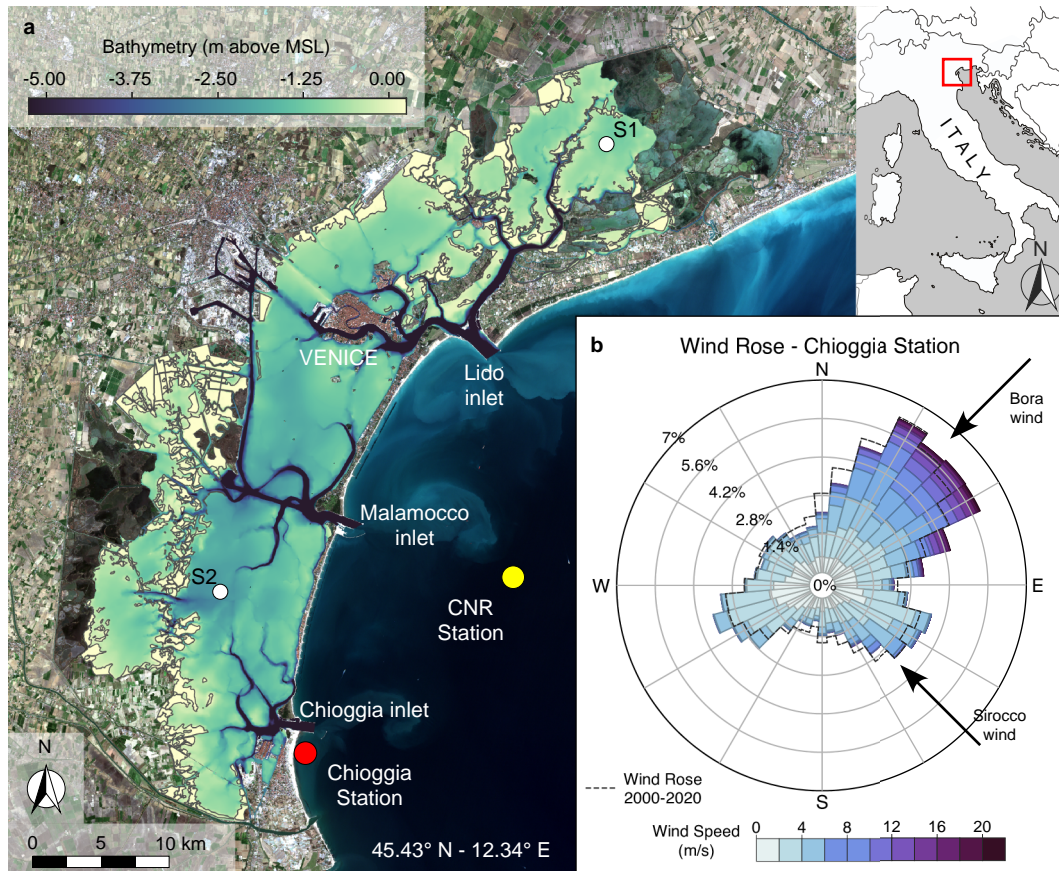


Figure 1. Morphological features and wind conditions characterizing the Venice Lagoon. **a**, Bathymetry of the Venice Lagoon (Base satellite image: Copernicus Sentinel data 2020, <https://scihub.copernicus.eu/>). The locations of the anemometric (Chioggia) and oceanographic (CNR Oceanographic Platform) stations are also shown, together with the locations of the two stations (S1 and S2) for which we provide detailed statistical characterization of over-threshold events. **b**, Wind rose for the data recorded at the Chioggia station in 2005. Dashed line shows the wind rose for the period 2000-2020.

181 2.1 Numerical Model

182 The flow field and sediment transport in the six configurations of the Venice La-
 183 goon are computed by using a numerical model, consisting of three modules. The cou-
 184 pling of the hydrodynamic module with the wind-wave module (WWTM) describes the

185 hydrodynamic flow field together with the generation and propagation of wind waves (Carniello
186 et al., 2005, 2011), while the sediment transport and the bed evolution module (STABEM)
187 evaluates the sediment dynamics and the effects on the morphology (Carniello et al., 2012).
188 All modules share the same computational grid.

189 The hydrodynamic module solves the 2-D shallow water equations using a semi-
190 implicit staggered finite element method based on Galerkin’s approach (Defina, 2000;
191 Martini et al., 2004). The equations are suitably rewritten in order to deal with flood-
192 ing and drying processes in morphologically irregular domains. The Strickler equation
193 is used to evaluate the bottom shear stress induced by currents, τ_c , considering the case
194 of turbulent flow over a rough wall. Further, the hydrodynamic module provides the flow
195 field characteristic requested by the wind-wave module to simulate the generation and
196 propagation of wind waves.

197 The wind-wave module (Carniello et al., 2011) solves the wave action conservation
198 equation parametrized using the zero-order moment of the wave action spectrum in the
199 frequency domain (Holthuijsen et al., 1989). The peak wave period is related to the lo-
200 cal wind speed and water depth, and this empirical correlation function is used to de-
201 termine the spatial and temporal distribution of the wave period (Breugem & Holthui-
202 jsen, 2007; Carniello et al., 2011; Young & Verhagen, 1996). The bottom shear stress in-
203 duced by wind waves, τ_{ww} , is computed as a function of the maximum horizontal orbital
204 velocity at the bottom, which is related to the significant wave height through the lin-
205 ear theory. Owing to the non-linear interaction between the wave and current bound-
206 ary layers, the maximum bottom shear stress, τ_{wc} , is enhanced beyond the linear addi-
207 tion of the wave-alone and current-alone stresses: in the WWTM this is considered adopt-
208 ing the empirical formulation suggested by Soulsby (1995, 1997).

209 The sediment transport and bed evolution module (STABEM) is based on the so-
210 lution of the advection-diffusion equation and Exner’s equation (Carniello et al., 2012).
211 This module uses two size classes of sediments to describe the bed composition (i.e. non-
212 cohesive sand and cohesive mud), in order to consider the simultaneous presence of co-
213 hesive and non-cohesive sediment typically characterizing tidal lagoons (van Ledden et
214 al., 2004). The local mud content, which varies both in space and time, marks off the
215 transition between the cohesive and non-cohesive behaviour of a mixture, and, conse-
216 quently, determines the critical value for bottom shear stress, which is locally estimated

217 based on the critical values assumed for pure sand and pure mud. However, this task is
218 tough and site-specific, and, moreover, field data are often limited compared to the spa-
219 tial variability of bed composition. To address this issue, field surveys in the Venice La-
220 goon have been used to identify an empirical relationship between the local bed com-
221 position and both the local bottom elevation and the distance from the inlets. We re-
222 fer to Carniello et al. (2012) for further details.

223 Another peculiarity of the sediment transport module is the stochastic approach
224 chosen to model the near-threshold conditions for sediment entrainment. Indeed, in shal-
225 low tidal basins, resuspension events are periodically driven by bottom shear stresses that
226 slightly exceed the erosion threshold. The bottom shear stress, as well as the critical shear
227 stress, is very unsteady owing to the non-uniform flow velocity, wave characteristics and
228 small-scale bottom heterogeneity. Hence, following the stochastic approach suggested by
229 Grass (1970), both the total bottom shear stress, τ_{wc} , and the critical shear stress for
230 erosion, τ_c , are treated as random variables (τ'_{wc} , and τ'_c , respectively) with lognormal
231 distributions, and their expected values are those calculated by WWTM and STABEM.
232 Consequently, the erosion rate depends on the probability that τ_{wc} exceeds τ'_c (Carniello
233 et al., 2012).

234 These coupled numerical models were used to perform one-year-long simulations
235 within the six different computational grids representing the historical configuration of
236 the Venice Lagoon and the portion of the Adriatic Sea in front of it. Hourly tidal level
237 gauged at the Consiglio Nazionale delle Ricerche (CNR) Oceanographic Platform, located
238 in the Adriatic Sea offshore of the lagoon, and wind velocities and directions recorded
239 at the Chioggia anemometric station are imposed as boundary conditions (Figure 1).

240 All configurations were forced with tidal levels and wind climate measured during
241 the whole year 2005, as this year was selected as a representative year, being the prob-
242 ability distribution of wind speed at the Chioggia Station in 2005 the closest to the mean
243 annual probability distribution in the period 2000-2020 (Figure 1). Forcing all the his-
244 torical configurations of the Venice Lagoon with the same wind and tidal conditions en-
245 ables us to isolate the effects of the morphological modifications on the wind-wave field,
246 hydrodynamics and sediment dynamics.

247 Another important issue to consider when studying SSC dynamics in shallow tidal
248 environments is the presence of benthic and halophytic vegetation, which both shelters

249 the bed against the hydrodynamic action and increases the local critical shear stress for
250 erosion because of the presence of roots. While the presence of halophytic vegetation over
251 salt marshes is almost ubiquitous, reconstructing the presence of benthic vegetation on
252 the tidal flats is much more difficult even for the present configuration of the lagoon and
253 practically impossible for the ancient configurations (Goodwin et al., 2021). For the above
254 reasons and for the sake of homogeneity, the simulations of the present study neglect the
255 presence of benthic vegetation on the tidal flat and assume all salt-marsh platforms to
256 be completely vegetated in each configuration of the lagoon, thus neglecting sediment
257 resuspension over them (Christiansen et al., 2000; Temmerman et al., 2005).

258 **2.2 Peak Over Threshold Analysis of SSC**

259 Sediment transport dynamics in tidal environments are the results of the complex
260 interplay between hydrodynamic, biologic, and geomorphologic processes. This interplay
261 between different factors can be fully framed only by taking into account both its de-
262 terministic and stochastic components. As an example, Carniello et al. (2011) argued
263 that morphological dynamics in the Venice Lagoon are mostly linked to a few severe re-
264 suspension events induced by wind waves, whose dynamics are markedly stochastic in
265 the present configurations (A. D’Alpaos et al., 2013; Carniello et al., 2016). Measure-
266 ments confirm that high SSC events are also important sediment suppliers for salt marshes
267 (Tognin et al., 2021).

268 In the present work, we used the peak over threshold theory (POT) (Balkema &
269 de Haan, 1974) to analyze temporal and spatial dynamics of the total SSC at any loca-
270 tion within each selected configuration of the Venice lagoon. First, a minimum-intensity
271 threshold, C_0 , was chosen to identify the set of overthreshold events from the modeled
272 SSC record, and then a statistical analysis of interarrival times, durations and intensi-
273 ties of the exceedances of the threshold was carried out. The interarrival time is defined
274 as the time interval between two consecutive upcrossings of the threshold, the duration
275 of the events is the time elapsed between any upcrossing and the subsequent downcross-
276 ing of the threshold, and, finally, the intensity is calculated as the largest exceedance of
277 the threshold in the time-lapse between an upcrossing and the subsequent downcross-
278 ing. These three variables are characterized by means of their probability density func-
279 tions and the corresponding moments for any location in all the considered configura-
280 tions of the Venice Lagoon, in order to provide a complete description of the SSC pat-

281 tern. The nature of the stochastic processes can be determined by the analysis of the
282 interarrival times distribution. Indeed, resuspension events can be mathematically mod-
283 eled as a marked Poisson process if the interarrival times between subsequent exceedances
284 of the threshold, C_0 , are independent and exponentially distributed random variables.
285 In order to assess that over-threshold SSC events can be modeled as a Poisson process,
286 we performed the Kolmogorov-Smirnov (KS) goodness of fit test on the distribution of
287 the interarrival times. In our case, the sequence of random events that define a 1-D Pois-
288 son process along the time axis is associated with a vector of random marks that defines
289 the duration and intensity of each over-threshold event. Memorylessness is one of the
290 most interesting features of Poisson processes because it states that the number of events
291 observed in disjoint subperiods is an independent, Poisson-distributed random variable.
292 According to the extreme value theory, a Poisson process emerges from a stochastic sig-
293 nal whenever enough high censoring threshold is chosen (Cramér & Leadbetter, 1967).
294 However, as this present analysis is designed to remove only the weak resuspension events
295 induced by periodic tidal currents, the critical threshold is well below the maximum ob-
296 served values. As a consequence, the aim of the proposed analysis is to characterize the
297 bulk effect of morphologically meaningful SSC events, rather than to describe the ex-
298 treme events.

299 Notwithstanding the increasing popularity of Poisson processes for the analytical
300 modeling of the long-term evolution of geophysical processes controlled by stochastic drivers
301 in hydrological and geomorphological sciences (e.g., Rodriguez-Iturbe et al., 1987; D’Odorico
302 & Fagherazzi, 2003; Botter et al., 2013; Park et al., 2014; Bertassello et al., 2018), only
303 in the last few years this approach has been adopted for tidal systems (A. D’Alpaos et
304 al., 2013; Carniello et al., 2016) and the applications portray an encouraging framework.

305 **3 Results and Discussion**

306 The statistical characterization of suspended sediment dynamics is provided through
307 the analysis of the one-year-long time series of the computed SSC on the basis of the POT
308 method. The choice of the threshold value, C_0 , that identifies morphologically signifi-
309 cant over-threshold SSC events has to consider two opposite requirements. On the one
310 hand, stochastic sediment concentration generated by storm-induced wind waves can be
311 distinguished from tide-modulated daily concentration only if C_0 is large enough. On
312 the other hand, too high values of C_0 can lead to a non-informative analysis because of

313 the large number of events unaccounted for. In the following, we used a constant thresh-
 314 old, C_0 , equal to 40 mg l^{-1} , as suggested by Carniello et al. (2016) by analyzing avail-
 315 able in-situ SSC time series and performing a sensitivity analysis for the statistical anal-
 316 ysis of SSC events in the present configuration of the Venice Lagoon.

317 As a first step, the SSC time series provided by the numerical simulations were low-
 318 pass filtered by applying a moving average procedure with a time window of 6 hours, in
 319 order to preserve the tide-induced modulation of the signal but, at the same time, to re-
 320 move artificial upcrossing and downcrossing of the threshold, generated by short-term
 321 fluctuations.

322 The distributions of interarrival times, intensity of peak excess and durations ob-
 323 tained using the POT analysis are then compared with an exponential distribution per-
 324 forming the KS test with a significance level $\alpha = 0.05$. The KS test is replicated at each
 325 node of the computational grids reproducing the selected configurations and the results
 326 are shown in Figure 2, where we can identify three different situations:

- 327 1. SSC events cannot be described as a Poisson process, i.e. the KS test is not sat-
 328 isfied for interarrival times, in the dark blue areas;
- 329 2. SSC events are indeed a marked Poisson process because interarrival times, peak
 330 excesses and durations satisfy the KS test, and, thus, are exponentially distributed
 331 random variables, in the red areas;
- 332 3. SSC events still are a marked Poisson process but at least one between intensity
 333 and duration does not satisfy the KS test, i.e. although interarrival times follow
 334 an exponential distribution, at least one between intensity and duration does not,
 335 in the yellow areas.

336 The spatial distribution of mean interarrival times (Figure 3), mean intensities of
 337 peak excesses (Figure 4), and mean durations (Figure 5) of over-threshold events are shown
 338 at any location within each of the six historical configurations where SSC events can be
 339 modeled as a Poisson process (i.e., the KS test is verified for interarrival times at sig-
 340 nificance level $\alpha = 0.05$).

341 The area of the lagoon where over-thresholds SSC events cannot be modeled as Pois-
 342 son processes are mostly represented by salt marshes and tidal channels in all configu-
 343 rations (see dark blue areas in Figure 2), similarly to the results for erosion events (BSS)

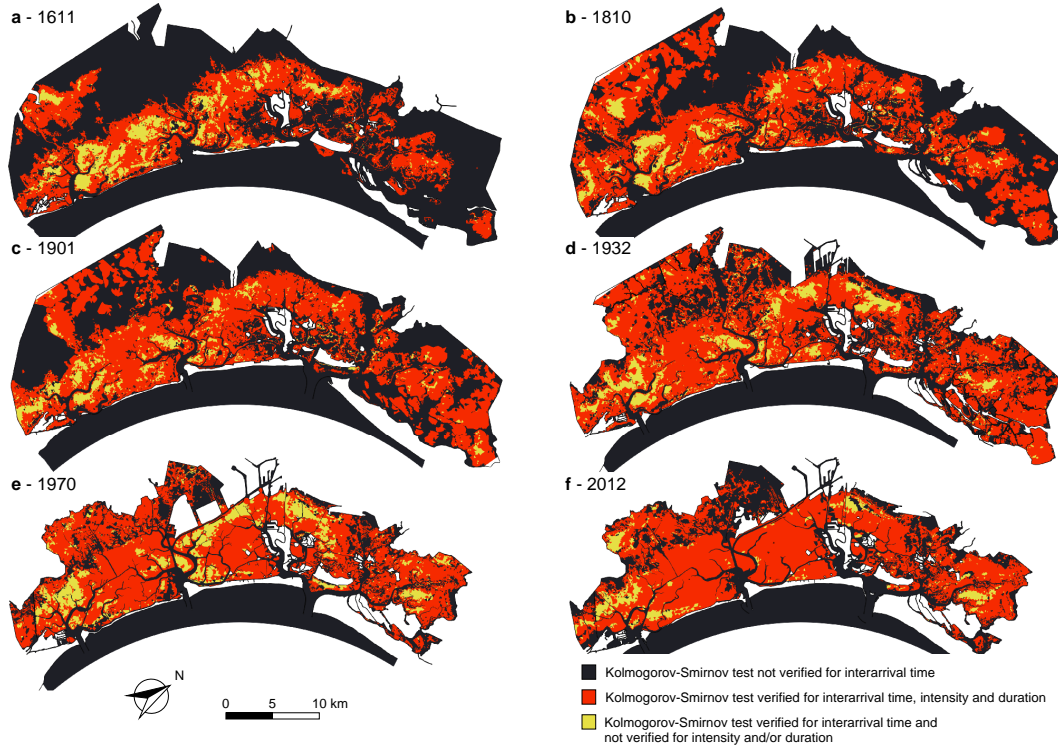


Figure 2. Kolmogorov-Smirnov test for overthreshold SSC events. Spatial distribution of Kolmogorov-Smirnov (KS) test at significance level ($\alpha = 0.05$) for the six different configurations of the Venice Lagoon: 1611 (a), 1810 (b), 1901 (c), 1932 (d), 1970 (e), and 2012 (f). In the maps we can distinguish areas where the KS test is: not verified (dark blue); verified for all the considered stochastic variables (interarrival time, intensity over the threshold and duration) (red); verified for the interarrival time and not for intensity and/or duration (yellow).

344 (A. D’Alpaos et al., Companion paper). On salt-marsh areas, both BSS and SSC thresh-
 345 olds (τ_C and C_0 respectively) are seldom exceeded (Figure S2 and S3), because the re-
 346 duced water depth over the marsh prevents the propagation of large wind waves and the
 347 presence of halophytic vegetation limits sediment advection by promoting deposition and
 348 stabilizes the bottom preventing erosion (e.g., Möller et al., 1999; Temmerman et al., 2005;
 349 Carniello et al., 2005). Within the main tidal channels and at the three inlets, as hap-
 350 pens for BSS, SSC dynamics are not Poissonian, but the reason why interarrival times
 351 of erosion and SSC events are not exponentially distributed are slightly different. In the
 352 main channel network and at the inlets, SSC exceeds the threshold value, C_0 , very few
 353 times or it does not exceed the threshold at all, due to vertical dispersion mechanisms
 354 that decrease the local concentration of sediment in suspension in deeper areas (Figure

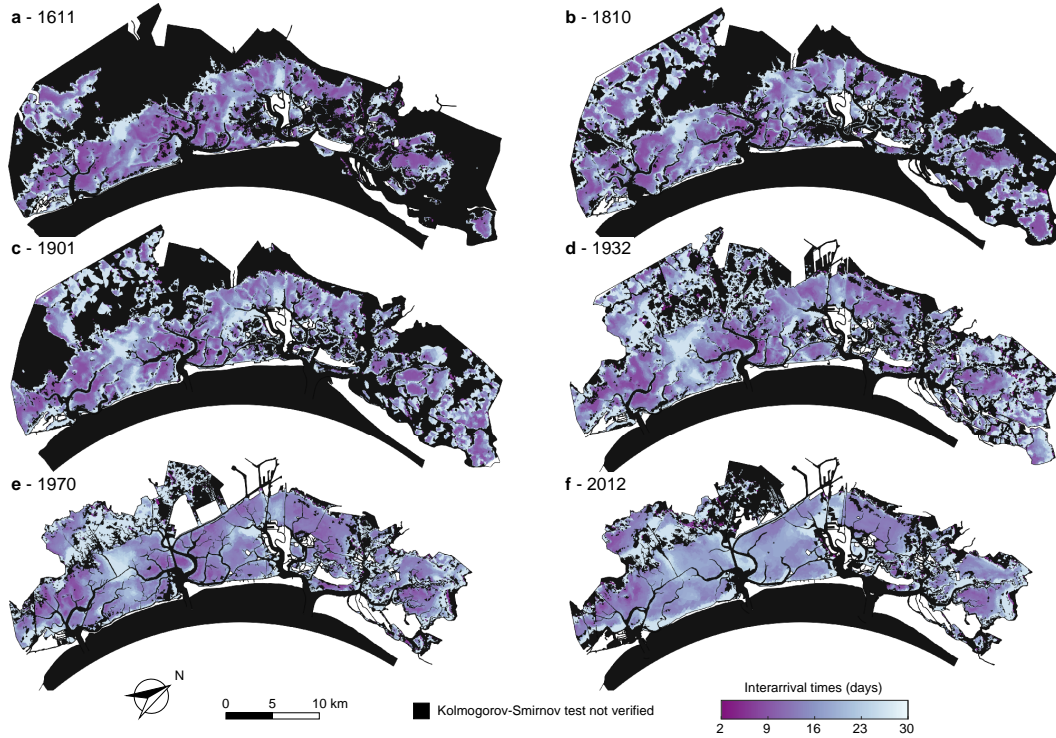


Figure 3. Mean interarrival time of overthreshold SSC events. Spatial distribution of mean interarrival times of over threshold exceedances at sites where SSC events can be modeled as a marked Poisson process, as confirmed by the KS test ($\alpha = 0.05$) for the six different configurations of the Venice Lagoon: 1611 (a), 1810 (b), 1901 (c), 1932 (d), 1970 (e), and 2012 (f).

355 S3). Conversely, BSS typically exceeds the threshold τ_c twice or four times a day (Fig-
 356 ure S2) mainly because of the tide action but the BSS time evolution cannot be mod-
 357 eled as a Poisson process as confirmed by the KS test on interarrival times of over-threshold
 358 BSS events (A. D’Alpaos et al., Companion paper).

359 However, SSC events can be modeled as a Poisson process over wide areas of the
 360 six configurations of the Venice Lagoon, in particular over tidal flats and subtidal plat-
 361 forms (see red and yellow areas in Figure 2). As a consequence, SSC dynamics can be
 362 effectively modeled by using a synthetic framework based on Poisson processes over widespread
 363 portions of the different morphological configurations experienced by the Venice Lagoon
 364 in the last four centuries.

365 Large interarrival times (i.e., larger than 30 days, Figure 3) are observed on tidal
 366 flats close to the main channel network because dilution processes within higher water

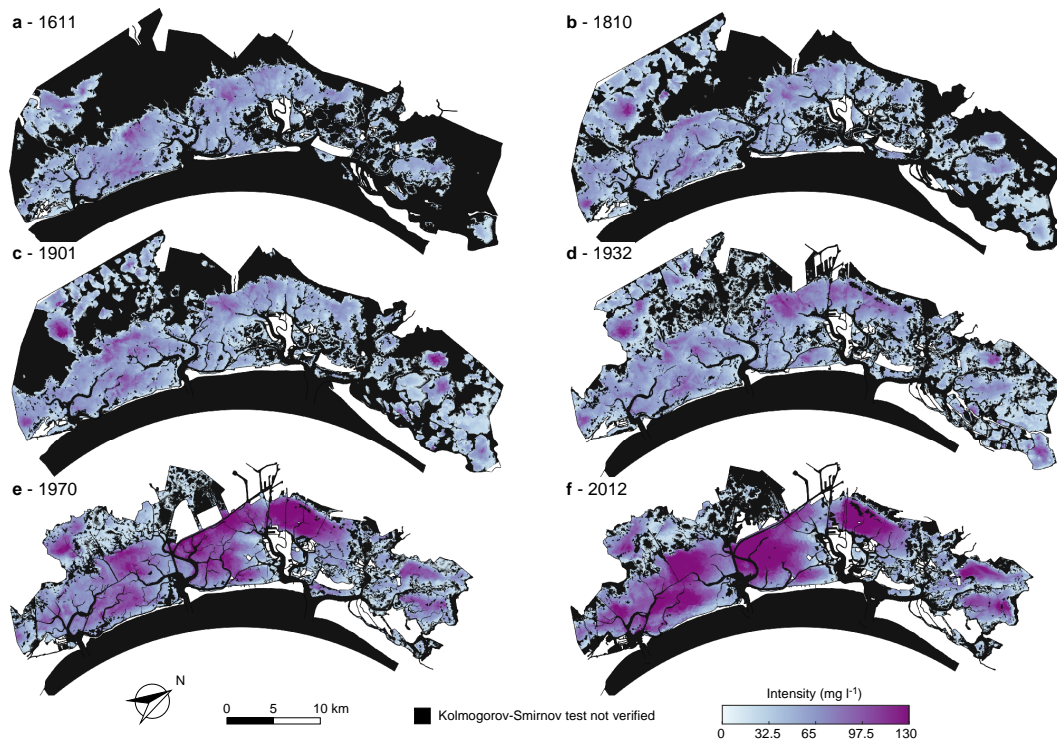


Figure 4. Mean intensity of overthreshold SSC events. Spatial distribution of mean intensity of peak excesses of over threshold exceedances at sites where SSC events can be modeled as a marked Poisson process, as confirmed by the KS test ($\alpha = 0.05$) for the six different configurations of the Venice Lagoon: 1611 (a), 1810 (b), 1901 (c), 1932 (d), 1970 (e), and 2012 (f).

367 depth, enhanced by the higher velocities in these sites, reduce sediment concentration,
 368 and hence only severe, but infrequent, events can lead to an exceedance of the thresh-
 369 old. Sheltered areas are also characterized by large interarrival times as represented by
 370 the northern portion of the lagoon, which is protected by the mainland from the north-
 371 easterly Bora wind, which is the most intense and morphologically significant wind in
 372 the Venice Lagoon (Figure 1b), and where the presence of extensive salt-marsh areas con-
 373 tinuously interrupts the propagation of wind waves. In this case, the reduced number
 374 of upcrossing events, and, consequently, large interarrival times is due to the sheltering
 375 action of salt marshes and islands in reducing wind-wave resuspension. SSC events over
 376 the marsh platform slightly changed through centuries. In the three oldest configurations
 377 (i.e., 1611, 1810 and 1901) mainly because of the wide extent of salt marshes, resuspen-
 378 sion events over salt marshes do not even reach the threshold, as shown by the number

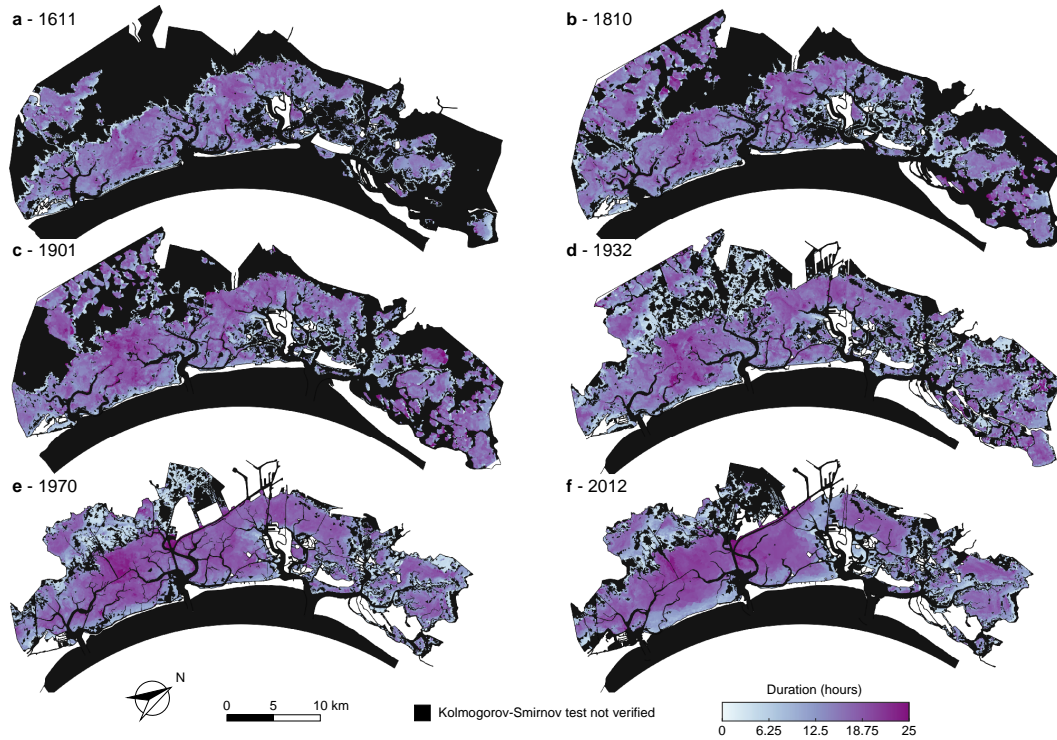


Figure 5. Mean durations of overthreshold SSC events. Spatial distribution of mean durations of over threshold exceedances at sites where SSC events can be modeled as a marked Poisson process, as confirmed by the KS test ($\alpha = 0.05$) for the six different configurations of the Venice Lagoon: 1611 (a), 1810 (b), 1901 (c), 1932 (d), 1970 (e), and 2012 (f).

379 of upcrossing (Figure S3). In the more recent ones, where salt-marsh extent importantly
 380 decreases, marshes start experiencing some over-threshold SSC events because of advec-
 381 tion of sediment from the adjacent areas, but the lower number of upcrossing allows the
 382 mean interarrival time assume large values.

383 Over wide tidal flat areas, where the threshold is exceeded in all the considered con-
 384 figurations, the mean interarrival time generally slightly increases through the centuries
 385 (Figure S5a). This trend is more evident in the central and southern parts of the lagoon,
 386 where, because of the deepening experienced in the last century, the number of events
 387 able to resuspend sediments from the bottom decreased importantly, hence increasing
 388 the mean interarrival time of intense SSC events. In fact, over the central-southern shal-
 389 low tidal flats of the four most ancient configurations, interarrival times present relatively
 390 low values (about 10 days), whereas they generally become longer (between 20 and 25
 391 days) in the same areas in the more recent configurations. On the contrary, in the bet-

392 ter preserved, northern portion of the lagoon, where the fetch is continuously interrupted
393 by islands, spits, and salt marshes also in the more recent configurations, the mean in-
394 terarrival times experienced only slight changes over centuries. As an example, Figure 6a
395 shows the mean interarrival times, λ_t , experienced by the “Palude Maggiore” tidal flat
396 (station S1 in Figure 1) that do not vary remarkably over time. On the contrary, the sub-
397 tidal flat at the watershed divide between the Chioggia and Malamocco inlets, known
398 as “Fondo dei Sette Morti” (station S2 in Figure 1), display a much larger variation of
399 λ_t with decreasing interarrival times through centuries (Figure 6d). In the more ancient
400 configurations, thanks to its relatively lower depth and its position sheltered by shallower
401 tidal flats, the station S2 experienced over-threshold events only during severe events.
402 In the more recent configurations, over-threshold events become more frequent due to
403 the deepening of the surrounding tidal flats, thus allowing larger waves and currents to
404 propagate in this area and enhancing resuspension as well as suspended sediment trans-
405 port.

406 The intensity of over-threshold events abruptly increases between 1932 and 1970
407 (Figure 4 and S5b). Indeed, SSC exceedance intensity maintains low mean values, gen-
408 erally below 60 mg l^{-1} , in all the configurations until 1932, thereafter it doubles on wide
409 tidal-flat areas, especially in the central-southern lagoon and northwest of the city of Venice,
410 where the action of wind waves is stronger because of the generalized deepening of those
411 areas. This analysis confirms that the intensity increase is much more important in the
412 central lagoon (station S2, Figure 6e) than in the northern part (station S1, Figure 6b).

413 Overall, over-threshold event durations slightly increase through the centuries (Fig-
414 ure 5 and S5c). However, two different trends can be distinguished in different portions
415 of the lagoon, likewise interarrival times and intensities. The duration increase in the more
416 pristine, northern portion of the basin is much lower than that in the central and south-
417 ern lagoon due to the heavier morphological modifications the latter areas experienced
418 (Figure 6c and f).

419 SSC dynamics are affected by local entrainment and advection/dispersion processes
420 from and toward the surrounding areas. Furthermore, the local resuspension is highly
421 influenced by the combined effect of tidal currents and wind waves, thus depending on
422 current velocity, water depth, fetch, wind intensity and duration (Fagherazzi & Wiberg,
423 2009; Carniello et al., 2016). As a consequence, the mean values of the random variables

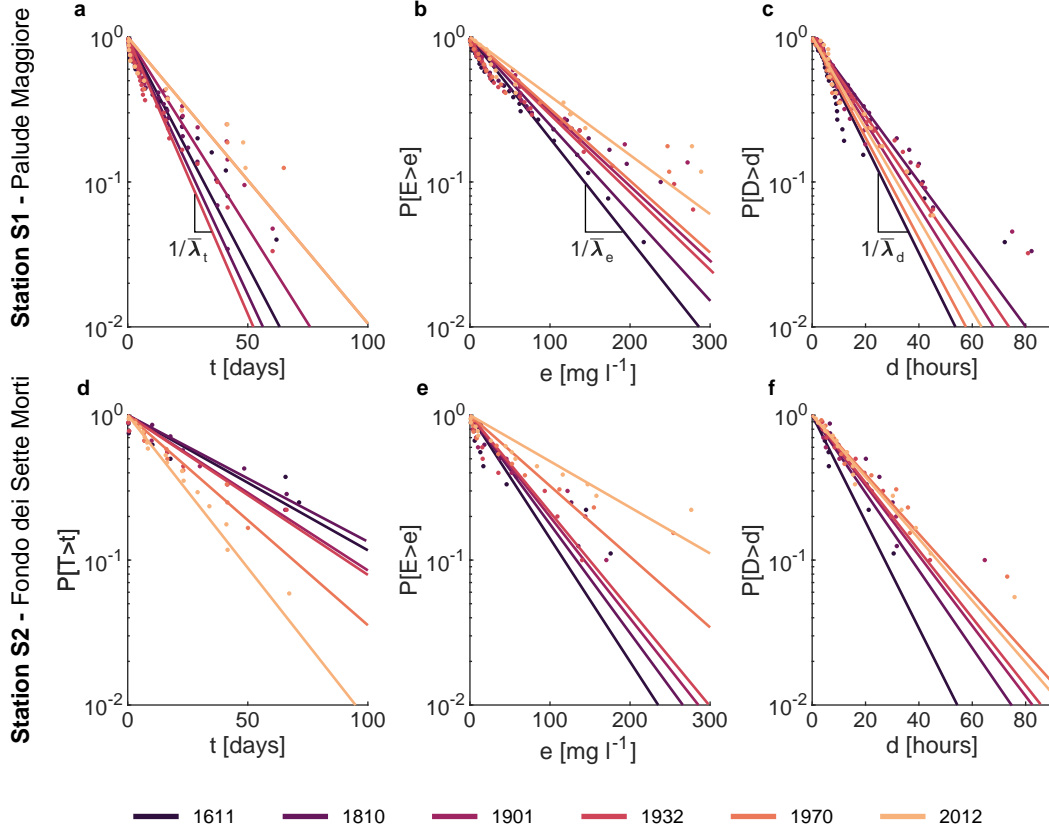


Figure 6. Overthreshold SSC events at stations S1 and S2. Statistical characterizations of over threshold events at two stations S1 “Palude Maggiore” and S2 “Fondo dei Sette Morti” (see Figure 1a for locations) in the six configurations of the Venice Lagoon. Probability distributions of (a-b) interarrival times, t ; (c-d) intensities of peak excesses of over threshold exceedances, e ; and (e-f) durations of over threshold event, d . $\bar{\lambda}_t$ mean interarrival time, $\bar{\lambda}_e$ mean peak excess intensity, and $\bar{\lambda}_d$ mean duration.

424 characterizing SSC events present highly heterogeneous spatial patterns in the more an-
 425 cient configurations of the Venice Lagoon due to their higher morphological complex-
 426 ity.

427 To describe the relationship between interarrival times, durations and intensities,
 428 the temporal cross-correlation between these three random variables was computed for
 429 each point within the six configurations of the Venice Lagoon (Figure S6, S7, S8). Du-
 430 ration of over threshold exceedances and intensity of peak excesses are highly correlated
 431 in all the six considered configurations, suggesting that longer events are linked to more

432 intense ones (Figure S6 and S9a). On the contrary, durations and interarrival times, as
433 well as intensities and interarrival times display almost no correlation (Figure S6, S7 and
434 S9b,c). These relations between interarrival time, intensity and duration back up the idea
435 that, as for BSS dynamics (A. D’Alpaos et al., Companion paper), over-threshold SSC
436 events can be modeled as a 3-D Poisson process in which the marks (intensity and du-
437 ration of over threshold events) are mutually dependent but independent on interarrival
438 times.

439 As a result of the cause-effect relationship between the BSS (cause) and SSC (ef-
440 fect), their spatial and temporal dynamics show a high cross-correlation between inter-
441 arrival times (Figure 7), intensity (Figure 8) and duration (Figure 9) of BSS and SSC
442 over-threshold events. Recalling the absence of correlation between interarrival times and
443 both intensities and durations for both BSS and SSC events, we can conclude that, when
444 generating synthetic time series, interarrival times of BSS and SSC events are mutually
445 dependent but not related to their intensity and duration. Intensities and durations of
446 SSC are instead strongly correlated with the corresponding properties of BSS events.

447 Despite showing high similarity and correlation, BSS and SSC events are not iden-
448 tical. The BSS ultimately depends on the local hydrodynamics, i.e. the local value of
449 the bed shear stress τ_{wc} produced by tidal currents and wind waves. On the contrary,
450 the SSC is not only a function of the local entrainment but also of the suspended sed-
451 iment flux from and towards the surrounding areas. As a result of the advection/dispersion
452 processes, the spatial pattern of SSC is smoother than that of BSS.

453 The statistical characterization of overthreshold SSC events using their mean in-
454 terarrival times, intensities and durations can be useful to estimate the total amount of
455 reworked sediments. Although different portions of the lagoon experience different trends
456 in these parameters depending on specific morphological modifications, a spatial aver-
457 age over the whole area where overthreshold SSC events can be described as Poisson pro-
458 cesses shows that globally mean interarrival times and duration slightly vary and remain
459 almost equal to about 30 days and 13 hours, respectively (Figure S5a and c). By con-
460 trast, intensity of the peak excess abruptly changes between 1932 and 1970. Between 1611
461 and 1932 the mean intensity maintains a value lower than 45 mg l^{-1} , but increases to 64
462 mg l^{-1} in 1970 and further to 73 mg l^{-1} in 2012 (Figure S5b).

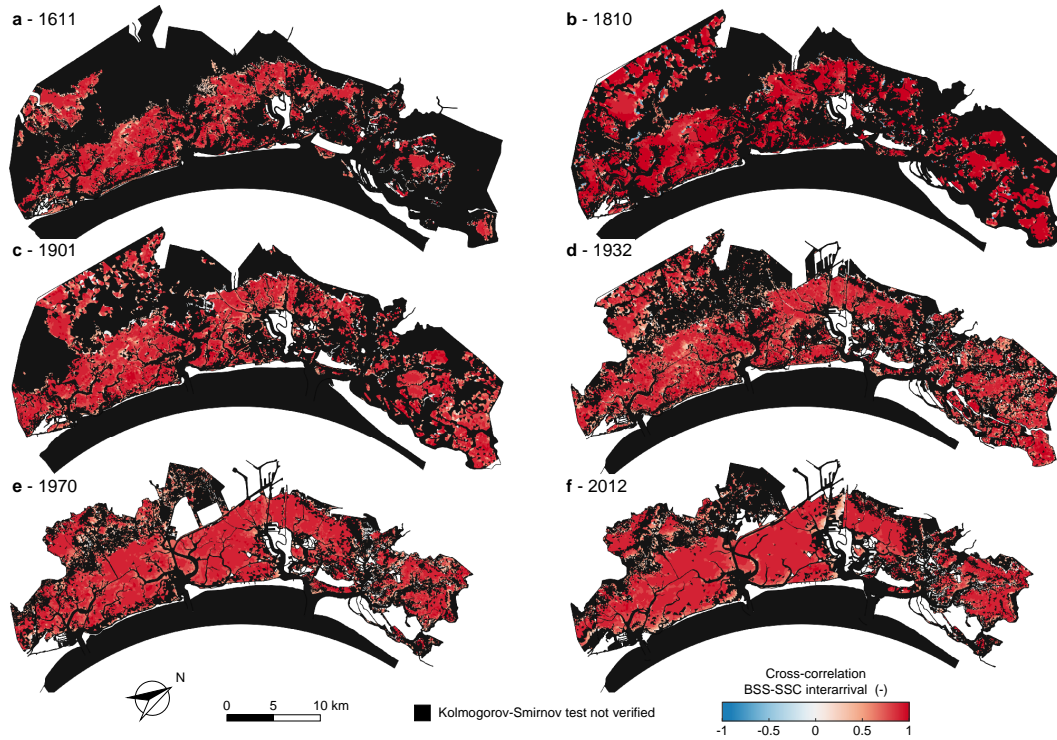


Figure 7. Cross-correlation between interarrival times of overthreshold BSS and SSC events. Spatial distribution of the cross-correlation between interarrival times of overthreshold BSS and SSC exceedances for the six different configurations of the Venice Lagoon: 1611 (a), 1810 (b), 1901 (c), 1932 (d), 1970 (e), and 2012 (f). Black identifies sites where overthreshold BSS or SSC events cannot be modeled as a marked Poisson process (i.e. the KS test is not verified for the interarrival time).

463 This increase in the intensity of overthreshold SSC events, clearly associated with
 464 the generalized deepening of the tidal-flat areas, generates an increase in the amount of
 465 reworked sediments. This means that on average every month, for about 13 hours, the
 466 amount of sediment mobilized within the basin increases from about $2 \cdot 10^6$ kg in the
 467 three most ancient configurations to more than $6.8 \cdot 10^6$ kg in the 2012 configuration
 468 (Table 1). Besides directly boosting the amount of sediment available for export toward
 469 the open sea given the ebb-dominated character of the Venice Lagoon (Ferrarin et al.,
 470 2015; Finotello et al., 2022), the increase of suspended sediment also affects numerous
 471 biological and ecological processes that in turn influence the morphological evolution of
 472 the tidal system (e.g., Venier et al., 2014; Pivato et al., 2019).

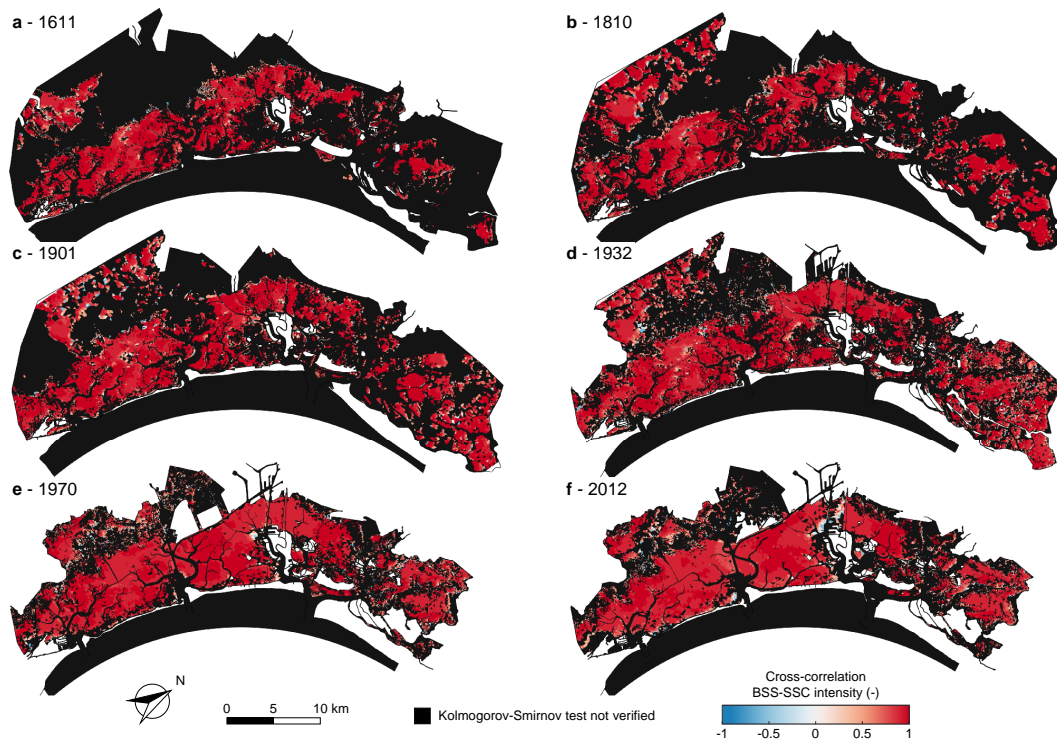


Figure 8. Cross-correlation between intensities of overthreshold BSS and SSC events. Spatial distribution of the cross-correlation between intensities of over threshold exceedances BSS and SSC for the six different configurations of the Venice Lagoon: 1611 (a), 1810 (b), 1901 (c), 1932 (d), 1970 (e), and 2012 (f). Black identifies sites where overthreshold BSS or SSC events cannot be modeled as a marked Poisson process (i.e. the KS test is not verified for the interarrival time).

473 As already mentioned, modeling the morphodynamic evolution of tidal landscapes
 474 over long timescales (decades or centuries) necessarily requires the use of simplified ap-
 475 proaches. However, a classical assumption of long-term evolution models is that the sed-
 476 iment supply is constant or monotonically related to mean water depth. The results pre-
 477 sented in this study, together with those obtained for erosion events (A. D’Alpaos et al.,
 478 Companion paper), demonstrate that the time series of both BSS and SSC can be de-
 479 scribed as marked Poisson processes with exponentially distributed interarrival times,
 480 intensities, and durations, thereby setting a framework for the synthetic generation of
 481 statistically significant external forcing factors (shear stress at the bottom and suspended
 482 sediment available in the water column) that should improve the reliability of long-term
 483 biomorphodynamic models with a limited increase in the number of parameters.

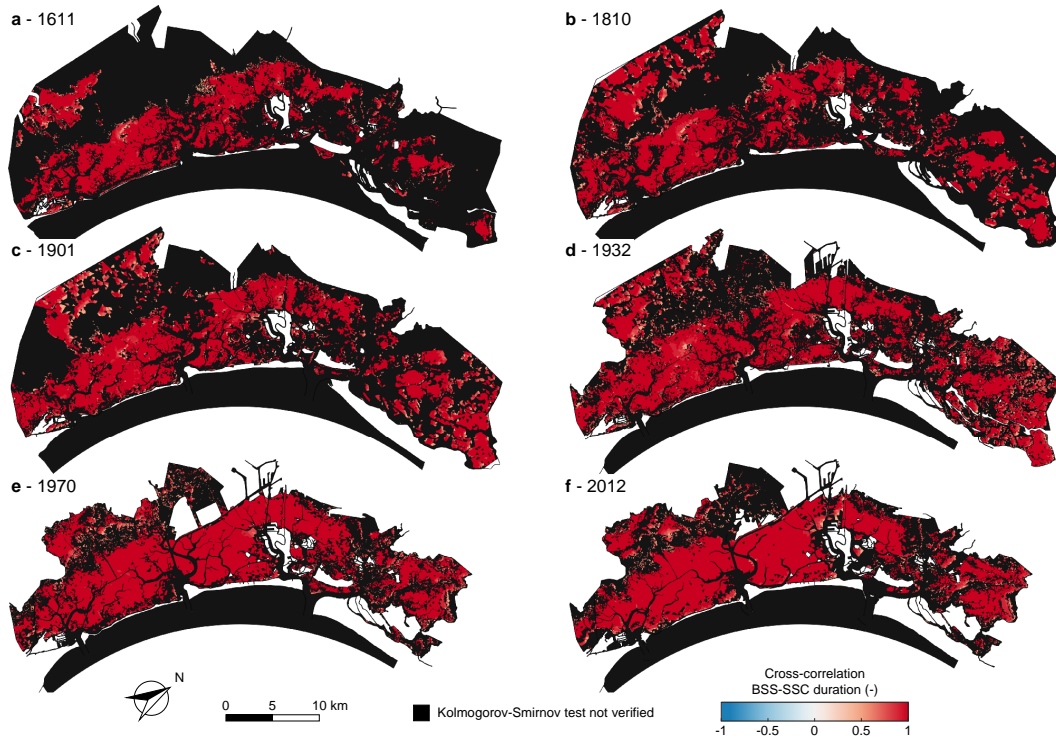


Figure 9. Cross-correlation between durations of overthreshold BSS and SSC events. Spatial distribution of the cross-correlation between durations of over threshold exceedances BSS and SSC for the six different configurations of the Venice Lagoon: 1611 (a), 1810 (b), 1901 (c), 1932 (d), 1970 (e), and 2012 (f). Black identifies sites where overthreshold BSS or SSC events cannot be modeled as a marked Poisson process (i.e. the KS test is not verified for the interarrival time).

484 4 Conclusions

485 SSC dynamics in shallow tidal environments is usually investigated by means of
 486 field measurements or remote sensing analysis. However, due to the limited spatial cov-
 487 erage of field measurement and the temporal resolution of satellite images, long-term SSC
 488 dynamics at basin scale are seldom available. Numerical models, once properly calibrated
 489 and tested, can provide reliable long SSC time series which can be used to statistically
 490 characterize the spatial and temporal variability of intense SSC events.

491 In the present study, we applied a custom-built, extensively tested, 2-D finite-element
 492 numerical model to reproduce SSC dynamics at basin scale in six historical configura-
 493 tions of the Venice Lagoon, covering a time span of four centuries. The computed SSC

Table 1. Sediment reworking in the historical configurations of the Venice Lagoon.

$area$ (km^2): area of the lagoon where KS is verified; h (m): mean water depth of the area; V_w ($10^6 m^3$): mean volume of water, obtained as product of area and water depth; e ($mg l^{-1}$): mean intensity of overthreshold SSC events; S_{mob} ($10^6 kg$): sediment mobilized, assuming a triangular-shaped temporal evolution of overthreshold SSC events, with peak excess e .

Year	area (km^2)	h (m)	V_w ($10^6 m^3$)	e ($mg l^{-1}$)	S_{mob} ($10^6 kg$)
1611	226.882	0.59	134.403	44.20	1.980
1810	294.649	0.43	127.022	40.84	1.729
1901	307.951	0.47	143.985	42.66	2.047
1932	350.166	0.54	188.661	43.49	2.734
1970	283.196	0.77	217.863	64.16	4.659
2012	270.022	1.04	279.969	73.21	6.832

494 time series were analysed on the basis of the Peak Over Threshold theory. Statistical anal-
 495 yses suggest that over-threshold SSC events can be modelled as a marked Poisson pro-
 496 cess over wide areas of all the selected configurations of the Venice Lagoon.

497 We found that, due to the morphological evolution experienced by the lagoon in
 498 the last four centuries, mean interarrival time, intensity and duration of overthreshold
 499 events generally increase through the centuries as a consequence of the morphological
 500 evolution of the shallow tidal environment, generating slightly less frequent and longer,
 501 but stronger, resuspension events.

502 Furthermore, almost no correlation is shown to exist between durations and inter-
 503 arrival times of over-threshold exceedances and between intensities and interarrival times,
 504 whereas the intensity of peak excesses and duration are highly correlated. This confirms
 505 that resuspension events can be modeled as a 3-D marked Poisson process with marks
 506 (intensity and duration) mutually dependent but independent on the interarrival times
 507 in all the historical configurations of the Venice Lagoon. Moreover, a comparison with
 508 the analysis of over-threshold BSS events shows that interarrival times, intensities and
 509 durations of both BSS and SSC events are mutually related.

510 These findings, together with those obtained for BSS events (A. D'Alpaos et al.,
511 Companion paper), provide the basis to develop a theoretical framework for generating
512 synthetic, yet statistically realistic, forcings to be used in the long-term morphodynamic
513 modeling of shallow tidal environments, in general, and for the Venice Lagoon, in par-
514 ticular.

515 **5 Open Research**

516 All data presented in this study and used for the analysis of the suspended sedi-
517 ment concentration are available at

518 <https://researchdata.cab.unipd.it/id/eprint/729>

519 [\(10.25430/researchdata.cab.unipd.it.00000729\)](https://researchdata.cab.unipd.it.00000729)

520 **Acknowledgments**

521 This scientific activity was partially performed as part of the Research Programme Venezia2021,
522 with contributions from the Provveditorato for the Public Works of Veneto, Trentino Alto
523 Adige and Friuli Venezia Giulia, provided through the concessionary of State Consorzio
524 Venezia Nuova and coordinated by CORILA, Research Line 3.2 (PI A.D.), by the 2019
525 University of Padova project (BIRD199419) ‘Tidal network ontogeny and evolution: a
526 comprehensive approach based on laboratory experiments with ancillary numerical mod-
527 elling and field measurements’ (PI L.C.), and by University of Padova SID2021 project,
528 ‘Unraveling Carbon Sequestration Potential by Salt-Marsh Ecosystems’ (P.I. A. D.).

529 The authors declare no competing interests.

530 **Author contributions**

531 Conceptualization: Davide Tognin, Andrea D’Alpaos, Andrea Rinaldo, Luca Carniello;

532 Methodology: Davide Tognin, Andrea D’Alpaos, Luca Carniello;

533 Formal analysis and investigation: Davide Tognin;

534 Figures: Davide Tognin;

535 Writing - original draft preparation: Davide Tognin;

536 Writing - review and editing: all authors;

537 Funding acquisition: Andrea D’Alpaos, Luca Carniello;

538 Resources: Andrea D’Alpaos, Luca Carniello, Luigi D’Alpaos, Andrea Rinaldo;

539 Supervision: Andrea D’Alpaos, Luca Carniello.

540 **References**

541 Anderson, F. E. (1972). Resuspension of estuarine sediments by small amplitude
542 waves. *Journal of Sedimentary Research*, 42(3), 602–607.

543 Balkema, A. A., & de Haan, L. (1974). Residual Life Time at Great Age. *The An-*
544 *nals of Probability*. doi: 10.1214/aop/1176996548

- 545 Bertassello, L. E., Rao, P. S. C., Park, J., Jawitz, J. W., & Botter, G. (2018).
 546 Stochastic modeling of wetland-groundwater systems. *Advances in Water Re-*
 547 *sources*, 112(December 2017), 214–223. doi: 10.1016/j.advwatres.2017.12.007
- 548 Botter, G., Basso, S., Rodriguez-Iturbe, I., & Rinaldo, A. (2013). Resilience of
 549 river flow regimes. *Proceedings of the National Academy of Sciences*, 110(32),
 550 12925–12930. doi: 10.1073/pnas.1311920110
- 551 Brand, E., Chen, M., & Montreuil, A.-L. (2020). Optimizing measurements of sed-
 552 iment transport in the intertidal zone. *Earth-Science Reviews*, 200, 103029.
 553 doi: 10.1016/j.earscirev.2019.103029
- 554 Breugem, W. A., & Holthuijsen, L. H. (2007). Generalized Shallow Water Wave
 555 Growth from Lake George. *Journal of Waterway, Port, Coastal, and Ocean*
 556 *Engineering*. doi: 10.1061/(asce)0733-950x(2007)133:3(173)
- 557 Carniello, L., D’Alpaos, A., Botter, G., & Rinaldo, A. (2016). Statistical character-
 558 ization of spatiotemporal sediment dynamics in the Venice lagoon. *Journal of*
 559 *Geophysical Research: Earth Surface*, 1049–1064. doi: 10.1002/2015JF003793
- 560 Carniello, L., D’Alpaos, A., & Defina, A. (2011). Modeling wind waves and tidal
 561 flows in shallow micro-tidal basins. *Estuarine, Coastal and Shelf Science*,
 562 92(2), 263–276. doi: 10.1016/j.ecss.2011.01.001
- 563 Carniello, L., Defina, A., & D’Alpaos, L. (2009). Morphological evolution of the
 564 Venice lagoon: Evidence from the past and trend for the future. *Journal of*
 565 *Geophysical Research*, 114(F4), F04002. doi: 10.1029/2008JF001157
- 566 Carniello, L., Defina, A., & D’Alpaos, L. (2012). Modeling sand-mud transport
 567 induced by tidal currents and wind waves in shallow microtidal basins: Ap-
 568 plication to the Venice Lagoon (Italy). *Estuarine, Coastal and Shelf Science*,
 569 102-103, 105–115. doi: 10.1016/j.ecss.2012.03.016
- 570 Carniello, L., Defina, A., Fagherazzi, S., & D’Alpaos, L. (2005). A combined wind
 571 wave-tidal model for the Venice lagoon, Italy. *Journal of Geophysical Research:*
 572 *Earth Surface*, 110(4), 1–15. doi: 10.1029/2004JF000232
- 573 Carniello, L., Silvestri, S., Marani, M., D’Alpaos, A., Volpe, V., & Defina, A. (2014).
 574 Sediment dynamics in shallow tidal basins: In situ observations, satellite re-
 575 trievals, and numerical modeling in the Venice Lagoon. *Journal of Geophysical*
 576 *Research: Earth Surface*, 119(4), 802–815. doi: 10.1002/2013JF003015
- 577 Carr, J. A., D’Odorico, P., McGlathery, K. J., & Wiberg, P. L. (2010). Stability and

- 578 bistability of seagrass ecosystems in shallow coastal lagoons: Role of feedbacks
 579 with sediment resuspension and light attenuation. *Journal of Geophysical*
 580 *Research: Biogeosciences*, 115(G3). doi: 10.1029/2009JG001103
- 581 Carr, J. A., D’Odorico, P., McGlathery, K. J., & Wiberg, P. L. (2016). Spatially
 582 explicit feedbacks between seagrass meadow structure, sediment and light:
 583 Habitat suitability for seagrass growth. *Advances in Water Resources*, 93,
 584 315–325. doi: <https://doi.org/10.1016/j.advwatres.2015.09.001>
- 585 Chen, X., Zhang, C., Paterson, D. M., Townend, I., Jin, C., Zhou, Z., . . . Feng, Q.
 586 (2019). The effect of cyclic variation of shear stress on non-cohesive sediment
 587 stabilization by microbial biofilms: the role of ‘biofilm precursors’. *Earth*
 588 *Surface Processes and Landforms*, 44(7), 1471–1481. doi: 10.1002/esp.4573
- 589 Christiansen, T., Wiberg, P. L., & Milligan, T. G. (2000). Flow and Sediment
 590 Transport on a Tidal Salt Marsh Surface. *Estuarine, Coastal and Shelf Sci-*
 591 *ence*, 50(3), 315–331. doi: 10.1006/ecss.2000.0548
- 592 Cramér, H., & Leadbetter, M. R. (1967). *Stationary and related stochastic processes*.
 593 New York: John Wiley & Sons, Ltd.
- 594 D’Alpaos, A., Carniello, L., & Rinaldo, A. (2013). Statistical mechanics of wind
 595 wave-induced erosion in shallow tidal basins: Inferences from the Venice La-
 596 goon. *Geophysical Research Letters*. doi: 10.1002/grl.50666
- 597 D’Alpaos, A., Lanzoni, S., Marani, M., & Rinaldo, A. (2007). Landscape evolution
 598 in tidal embayments: Modeling the interplay of erosion, sedimentation, and
 599 vegetation dynamics. *Journal of Geophysical Research*, 112(F1), F01008. doi:
 600 10.1029/2006JF000537
- 601 D’Alpaos, A., & Marani, M. (2016). Reading the signatures of biologic-geomorphic
 602 feedbacks in salt-marsh landscapes. *Advances in Water Resources*, 93, 265–
 603 275. doi: 10.1016/j.advwatres.2015.09.004
- 604 D’Alpaos, A., Mudd, S. M., & Carniello, L. (2011). Dynamic response of marshes
 605 to perturbations in suspended sediment concentrations and rates of relative sea
 606 level rise. *Journal of Geophysical Research: Earth Surface*, 116(4), 1–13. doi:
 607 10.1029/2011JF002093
- 608 D’Alpaos, A., Tognin, D., Tommasini, L., D’Alpaos, L., Rinaldo, A., & Carniello,
 609 L. (Companion paper). *Statistical characterization of erosion and sediment*
 610 *transport mechanics in shallow tidal environments. part 1: erosion dynamics*

- 611 [under review].
- 612 D'Alpaos, L. (2010). *Fatti e misfatti di idraulica lagunare. La laguna di Venezia*
 613 *dalla diversione dei fiumi alle nuove opere delle bocche di porto*. Venice: Istit-
 614 tuto Veneto di Scienze, Lettere e Arti.
- 615 Defina, A. (2000). Two-dimensional shallow flow equations for partially dry areas.
 616 *Water Resources Research*, *36*(11), 3251–3264. doi: 10.1029/2000WR900167
- 617 D'Odorico, P., & Fagherazzi, S. (2003). A probabilistic model of rainfall-triggered
 618 shallow landslides in hollows: A long-term analysis. *Water Resources Research*.
 619 doi: 10.1029/2002WR001595
- 620 Dyer, K. R. (1989). Sediment processes in estuaries: Future research require-
 621 ments. *Journal of Geophysical Research*, *94*(C10), 14327. doi: 10.1029/
 622 JC094iC10p14327
- 623 Dyer, K. R., Christie, M. C., Feates, N., Fennessy, M. J., Pejrup, M., & van der Lee,
 624 W. (2000). An Investigation into Processes Influencing the Morphodynamics
 625 of an Intertidal Mudflat, the Dollard Estuary, The Netherlands: I. Hydrody-
 626 namics and Suspended Sediment. *Estuarine, Coastal and Shelf Science*, *50*(5),
 627 607–625. doi: 10.1006/ecss.1999.0596
- 628 Fagherazzi, S., & Wiberg, P. L. (2009). Importance of wind conditions, fetch, and
 629 water levels on wave-generated shear stresses in shallow intertidal basins. *Jour-
 630 nal of Geophysical Research: Earth Surface*. doi: 10.1029/2008JF001139
- 631 Ferrarin, C., Tomasin, A., Bajo, M., Petrizzo, A., & Umgiesser, G. (2015). Tidal
 632 changes in a heavily modified coastal wetland. *Continental Shelf Research*,
 633 *101*, 22–33. doi: 10.1016/j.csr.2015.04.002
- 634 Finotello, A., Tognin, D., Carniello, L., Ghinassi, M., Bertuzzo, E., & D'Alpaos,
 635 A. (2022). Hydrodynamic feedbacks of salt-marsh loss in shallow microti-
 636 dal back-barrier systems. *Earth and Space Science Open Archive*, *32*. doi:
 637 10.1002/essoar.10511787.2
- 638 Friedrichs, C. T., & Madsen, O. S. (1992). Nonlinear diffusion of the tidal signal in
 639 frictionally dominated embayments. *Journal of Geophysical Research*, *97*(C4),
 640 5637. doi: 10.1029/92jc00354
- 641 Gartner, J. W. (2004). Estimating suspended solids concentrations from
 642 backscatter intensity measured by acoustic Doppler current profiler in
 643 San Francisco Bay, California. *Marine Geology*, *211*(3-4), 169–187. doi:

644 10.1016/j.margeo.2004.07.001

645 Goodwin, G. C. H., Carniello, L., D'Alpaos, A., Marani, M., & Silvestri, S. (2021).

646 Long-term seasonal dynamics of seagrass extent in a Mediterranean Lagoon

647 (Venice, Italy) from public satellite data. In *Egu general assembly conference*.

648 Copernicus Meetings. doi: <https://doi.org/10.5194/egusphere-egu21-8837>

649 Grass, A. J. (1970). Initial Instability of Fine Bed Sand. *Journal of the Hydraulics*

650 *Division*, 96(3), 619–632. doi: 10.1061/JYCEAJ.0002369

651 Green, M. O. (2011). Very small waves and associated sediment resuspension on an

652 estuarine intertidal flat. *Estuarine, Coastal and Shelf Science*, 93(4), 449–459.

653 doi: 10.1016/j.ecss.2011.05.021

654 Green, M. O., Black, K. P., & Amos, C. L. (1997). Control of estuarine sediment

655 dynamics by interactions between currents and waves at several scales. *Marine*

656 *Geology*, 144(1-3), 97–116. doi: 10.1016/S0025-3227(97)00065-0

657 Green, M. O., & Coco, G. (2007). Sediment transport on an estuarine inter-

658 tidal flat: Measurements and conceptual model of waves, rainfall and ex-

659 changes with a tidal creek. *Estuarine, Coastal and Shelf Science*. doi:

660 10.1016/j.ecss.2006.11.006

661 Green, M. O., & Coco, G. (2014). Review of wave-driven sediment resuspension and

662 transport in estuaries. *Reviews of Geophysics*, 52(1), 77–117. doi: 10.1002/

663 2013RG000437

664 Holthuijsen, L. H., Booij, N., & Herbers, T. H. C. (1989). A prediction model for

665 stationary, short-crested waves in shallow water with ambient currents. *Coastal*

666 *Engineering*, 13(1), 23–54. doi: [https://doi.org/10.1016/0378-3839\(89\)90031](https://doi.org/10.1016/0378-3839(89)90031)

667 -8

668 Hughes, Z. J. (2012). Tidal Channels on Tidal Flats and Marshes. In R. Davis

669 & R. Dalrymple (Eds.), *Principles of tidal sedimentology* (pp. 1–621). doi: 10

670 .1007/978-94-007-0123-6

671 Kirwan, M. L., & Murray, A. B. (2007). A coupled geomorphic and ecological

672 model of tidal marsh evolution. *Proceedings of the National Academy*

673 *of Sciences of the United States of America*, 104(15), 6118–6122. doi:

674 10.1073/pnas.0700958104

675 Lawson, S. E., Wiberg, P. L., McGlathery, K. J., & Fugate, D. C. (2007). Wind-

676 driven sediment suspension controls light availability in a shallow coastal

- 677 lagoon. *Estuaries and Coasts*, *30*(1), 102–112. doi: 10.1007/BF02782971
- 678 Le Hir, P., Monbet, Y., & Orvain, F. (2007). Sediment erodability in sediment trans-
679 port modelling: Can we account for biota effects? *Continental Shelf Research*,
680 *27*(8), 1116–1142. doi: 10.1016/j.csr.2005.11.016
- 681 Maciel, F. P., Santoro, P. E., & Pedocchi, F. (2021). Spatio-temporal dynamics of
682 the Río de la Plata turbidity front; combining remote sensing with in-situ mea-
683 surements and numerical modeling. *Continental Shelf Research*, *213*, 104301.
684 doi: <https://doi.org/10.1016/j.csr.2020.104301>
- 685 Marani, M., Da Lio, C., & D’Alpaos, A. (2013). Vegetation engineers marsh mor-
686 phology through multiple competing stable states. *Proceedings of the National
687 Academy of Sciences*. doi: 10.1073/pnas.1218327110
- 688 Martini, P., Carniello, L., & Avanzi, C. (2004). Two dimensional modelling of flood
689 flows and suspended sediment transport: the case of the Brenta River, Veneto
690 (Italy). *Natural Hazards and Earth System Sciences*, *4*(1), 165–181. doi:
691 10.5194/nhess-4-165-2004
- 692 Masselink, G., Hughes, M., & Knight, J. (2014). *Introduction to Coastal Processes
693 and Geomorphology*. Routledge. doi: 10.4324/9780203785461
- 694 McSweeney, J. M., Chant, R. J., Wilkin, J. L., & Sommerfield, C. K. (2017).
695 Suspended-Sediment Impacts on Light-Limited Productivity in the Delaware
696 Estuary. *Estuaries and Coasts*, *40*(4), 977–993. doi: 10.1007/s12237-016-0200
697 -3
- 698 Miller, R. L., & McKee, B. A. (2004). Using MODIS Terra 250 m imagery to map
699 concentrations of total suspended matter in coastal waters. *Remote Sensing of
700 Environment*, *93*(1), 259–266. doi: <https://doi.org/10.1016/j.rse.2004.07.012>
- 701 Möller, I., Spencer, T., French, J. R., Leggett, D. J., & Dixon, M. (1999). Wave
702 transformation over salt marshes: A field and numerical modelling study
703 from north Norfolk, England. *Estuarine, Coastal and Shelf Science*. doi:
704 10.1006/ecss.1999.0509
- 705 Moore, K. A., & Wetzel, R. L. (2000). Seasonal variations in eelgrass (*Zostera
706 marina* L.) responses to nutrient enrichment and reduced light availability
707 in experimental ecosystems. *Journal of Experimental Marine Biology and
708 Ecology*, *244*(1), 1–28. doi: [https://doi.org/10.1016/S0022-0981\(99\)00135-5](https://doi.org/10.1016/S0022-0981(99)00135-5)
- 709 Murray, A. B. (2007). Reducing model complexity for explanation and prediction.

- 710 *Geomorphology*, 90(3-4), 178–191. doi: 10.1016/j.geomorph.2006.10.020
- 711 Nepf, H. M. (1999, 2). Drag, turbulence, and diffusion in flow through emer-
712 gent vegetation. *Water Resources Research*, 35(2), 479–489. doi: 10.1029/
713 1998WR900069
- 714 Nichols, M. M., & Boon, J. D. (1994). Sediment Transport Processes in Coastal
715 Lagoons. In B. Kjerfve (Ed.), *Coastal lagoon processes* (Vol. 60, pp. 157–219).
716 doi: 10.1016/S0422-9894(08)70012-6
- 717 Ouillon, S., Douillet, P., & Andréfouët, S. (2004). Coupling satellite data with
718 in situ measurements and numerical modeling to study fine suspended sedi-
719 ment transport: a study for the lagoon of New Caledonia. *Coral Reefs*, 23(1),
720 109–122. doi: 10.1007/s00338-003-0352-z
- 721 Park, J., Botter, G., Jawitz, J. W., & Rao, P. S. C. (2014). Stochastic modeling
722 of hydrologic variability of geographically isolated wetlands: Effects of hydro-
723 climatic forcing and wetland bathymetry. *Advances in Water Resources*. doi:
724 10.1016/j.advwatres.2014.03.007
- 725 Parsons, D. R., Schindler, R. J., Hope, J. A., Malarkey, J., Baas, J. H., Peakall,
726 J., ... Thorne, P. D. (2016). The role of biophysical cohesion on subaque-
727 ous bed form size. *Geophysical Research Letters*, 43(4), 1566–1573. doi:
728 10.1002/2016GL067667
- 729 Pivato, M., Carniello, L., Moro, I., & D’Odorico, P. (2019). On the feedback be-
730 tween water turbidity and microphytobenthos growth in shallow tidal envi-
731 ronments. *Earth Surface Processes and Landforms*, 44(5), 1192–1206. doi:
732 10.1002/esp.4567
- 733 Ralston, D. K., & Stacey, M. T. (2007). Tidal and meteorological forcing of sed-
734 iment transport in tributary mudflat channels. *Continental Shelf Research*,
735 27(10-11), 1510–1527. doi: 10.1016/j.csr.2007.01.010
- 736 Rodriguez-Iturbe, I., Cox, D. R., & Isham, V. (1987). Some models for rainfall
737 based on stochastic point processes. *Proceedings of the Royal Society of*
738 *London. A. Mathematical and Physical Sciences*, 410(1839), 269–288. doi:
739 10.1098/rspa.1987.0039
- 740 Roner, M., D’Alpaos, A., Ghinassi, M., Marani, M., Silvestri, S., Franceschinis, E., &
741 Realdon, N. (2016). Spatial variation of salt-marsh organic and inorganic de-
742 position and organic carbon accumulation: Inferences from the Venice lagoon,

- Italy. *Advances in Water Resources*. doi: 10.1016/j.advwatres.2015.11.011
- Ruhl, C. A., Schoellhamer, D. H., Stumpf, R. P., & Lindsay, C. L. (2001). Combined Use of Remote Sensing and Continuous Monitoring to Analyse the Variability of Suspended-Sediment Concentrations in San Francisco Bay, California. *Estuarine, Coastal and Shelf Science*, 53(6), 801–812. doi: 10.1006/ecss.2000.0730
- Sanford, L. P. (1994). Wave-Forced Resuspension of Upper Chesapeake Bay Muds. *Estuaries*, 17(1), 148. doi: 10.2307/1352564
- Sarretta, A., Pillon, S., Molinaroli, E., Guerzoni, S., & Fontolan, G. (2010). Sediment budget in the Lagoon of Venice, Italy. *Continental Shelf Research*, 30(8), 934–949. doi: 10.1016/j.csr.2009.07.002
- Soulsby, R. L. (1995). Bed shear-stresses due to combined waves and currents. In M. J. F. Stive (Ed.), *Advances in coastal morphodynamics* (p. 420-423). Delft Hydraul., Delft, Netherlands.
- Soulsby, R. L. (1997). *Dynamics of Marine Sands: A Manual for Practical Applications*. Thomas Telford, London.
- Tambroni, N., Figueiredo da Silva, J., Duck, R. W., McLelland, S. J., Venier, C., & Lanzoni, S. (2016). Experimental investigation of the impact of macroalgal mats on the wave and current dynamics. *Advances in Water Resources*, 93, 326–335. doi: 10.1016/j.advwatres.2015.09.010
- Temmerman, S., Bouma, T. J., Govers, G., & Lauwaet, D. (2005). Flow paths of water and sediment in a tidal marsh: Relations with marsh developmental stage and tidal inundation height. *Estuaries*, 28(3), 338–352. doi: 10.1007/BF02693917
- Temmerman, S., Bouma, T. J., Van De Koppel, J., van der Wal, D., de Vries, M. B., & Herman, P. M. J. (2007). Vegetation causes channel erosion in a tidal landscape. *Geology*, 35(7), 631–634. doi: 10.1130/G23502A.1
- Tinoco, R. O., & Coco, G. (2016). A laboratory study on sediment resuspension within arrays of rigid cylinders. *Advances in Water Resources*, 92, 1–9. doi: 10.1016/j.advwatres.2016.04.003
- Tognin, D., D’Alpaos, A., Marani, M., & Carniello, L. (2021). Marsh resilience to sea-level rise reduced by storm-surge barriers in the Venice Lagoon. *Nature Geoscience*, 14(12), 906–911. doi: 10.1038/s41561-021-00853-7
- Tognin, D., Finotello, A., D’Alpaos, A., Viero, D. P., Pivato, M., Mel, R. A., . . .

- 776 Carniello, L. (2022). Loss of geomorphic diversity in shallow tidal embayments
777 promoted by storm-surge barriers. *Science Advances*, 8(13), eabm8446. doi:
778 10.1126/sciadv.abm8446
- 779 Tommasini, L., Carniello, L., Ghinassi, M., Roner, M., & D'Alpaos, A. (2019).
780 Changes in the wind-wave field and related salt-marsh lateral erosion:
781 inferences from the evolution of the Venice Lagoon in the last four cen-
782 turies. *Earth Surface Processes and Landforms*, 44(8), 1633–1646. doi:
783 doi:10.1002/esp.4599
- 784 van Ledden, M., Wang, Z. B., Winterwerp, H., & De Vriend, H. J. (2004). Sand-
785 mud morphodynamics in a short tidal basin. In *Ocean dynamics*. doi: 10.1007/
786 s10236-003-0050-y
- 787 Venier, C., D'Alpaos, A., & Marani, M. (2014). Evaluation of sediment prop-
788 erties using wind and turbidity observations in the shallow tidal areas of
789 the Venice Lagoon. *Journal of Geophysical Research: Earth Surface*. doi:
790 10.1002/2013JF003019
- 791 Volpe, V., Silvestri, S., & Marani, M. (2011). Remote sensing retrieval of suspended
792 sediment concentration in shallow waters. *Remote Sensing of Environment*,
793 115(1), 44–54. doi: 10.1016/j.rse.2010.07.013
- 794 Vu, H. D., Wieski, K., & Pennings, S. C. (2017). Ecosystem engineers drive creek
795 formation in salt marshes. *Ecology*, 98(1), 162–174. doi: 10.1002/ecy.1628
- 796 Wang, P. (2012). Principles of Sediment Transport Applicable in Tidal Environ-
797 ments. In R. A. Davis & R. W. Dalrymple (Eds.), *Principles of tidal sedimen-*
798 *tology* (Vol. c, pp. 1–621). Dordrecht: Springer Netherlands. doi: 10.1007/978
799 -94-007-0123-6
- 800 Widdows, J., & Brinsley, M. (2002). Impact of biotic and abiotic processes on
801 sediment dynamics and the consequences to the structure and function-
802 ing of the intertidal zone. *Journal of Sea Research*, 48(2), 143–156. doi:
803 10.1016/S1385-1101(02)00148-X
- 804 Woodroffe, C. D. (2002). *Coasts*. Cambridge: Cambridge University Press. doi: 10
805 .1017/CBO9781316036518
- 806 Wren, D. G., Barkdoll, B. D., Kuhnle, R. A., & Derrow, R. W. (2000). Field Tech-
807 niques for Suspended-Sediment Measurement. *Journal of Hydraulic Engineer-*
808 *ing*, 126(2), 97–104. doi: 10.1061/(ASCE)0733-9429(2000)126:2(97)

809 Young, I. R., & Verhagen, L. A. (1996). The growth of fetch limited waves in water
810 of finite depth. Part 1. Total energy and peak frequency. *Coastal Engineering*.
811 doi: 10.1016/S0378-3839(96)00006-3